HHS Public Access

Author manuscript

Carbohydr Polym. Author manuscript; available in PMC 2020 May 01.

Published in final edited form as:

Carbohydr Polym. 2019 May 01; 211: 141–151. doi:10.1016/j.carbpol.2019.02.010.

Migration and proliferation of cancer cells in culture are differentially affected by molecular size of modified citrus pectin

Samira Bernardino Ramos do Prado[a], **Tânia Misuzu Shiga**[a], **Yosuke Harazono**[b,c], **Victor A. Hogan**[b], **Avraham Raz**[b], **Nicholas C. Carpita**[d], **João Paulo Fabi**[a,e,f,*]

[a]Department of Food Science and Experimental Nutrition, School of Pharmaceutical Sciences, University of São Paulo, São Paulo, SP, Brazil

[b]Departments of Oncology and Pathology, School of Medicine, Wayne State University, and Karmanos Cancer Institute, Detroit, MI, USA

[c]Department of Maxillofacial Surgery, Tokyo Medical and Dental University, Bunkyo-ku, Tokyo, Japan

[d]Department of Botany & Plant Pathology, Purdue University, West Lafayette, IN, USA

[e]Food and Nutrition Research Center (NAPAN), University of São Paulo, São Paulo, SP, Brazil

[f]Food Research Center (FoRC), CEPID-FAPESP (Research, Innovation and Dissemination Centers, São Paulo Research Foundation), São Paulo, SP, Brazil

Abstract

While chemically and thermally modified citrus pectin (MCP) has already been studied for health benefits, it is unknown how size-fractionated oligo- and polysaccharides differentially affect cancer cell behavior. We produced thermally MCP and fractionated it by molecular size to evaluate the effect these polymers have on cancer cells. MCP30/10 (between 30 and 10kDa) had more esterified homogalacturonans (HG) and fewer rhamnogalacturonans (RG-I) than MCP and MCP30 (higher than 30kDa), while MCP10/3 (between 10 and 3kDa) showed higher amounts of type I arabinogalactans (AGI) and lower amounts of RG-I. MCP3 (smaller than 3 kDa) presented less esterified HG and the lowest amount of AGI and RG-I. Our data indicate that the enrichment of de-esterified HG oligomers and the AGI and RG-I depletions in MCP3, or the increase of AGI and loss of RGI in MCP30/10, enhance the anticancer behaviors by inhibiting migration, aggregation, and proliferation of cancer cells.

Keywords

Pectin; Modified pectin; Citrus; Cancer cells

[*]Corresponding author at: Avenida Professor Lineu Prestes, 580, bloco 14, 05588-000, São Paulo, SP, Brazil. samiraprado@usp.br (S.B.R. do Prado), tatymish@usp.br (T.M. Shiga), yousuke.harazono.xz@east.ntt.co.jp (Y. Harazono), hoganv@karmanos.org (V.A. Hogan), raza@karmanos.org (A. Raz), carpita@purdue.edu (N.C. Carpita), jpfabi@usp.br (J.P. Fabi).

Appendix A. Supplementary data

Supplementary material related to this article can be found, in the online version, at doi:https://doi.org/10.1016/j.carbpol.2019.02.010.

1. Introduction

Previous studies have supported an association between a dietary fiber (DF)-rich diet and a reduced risk of colorectal cancer (O'Keefe, 2016; Vieira et al., 2017). However, the biological mechanism for how DF acts to reduce the chance of intestinal cells altering to cancerous phenotypes is not fully understood.

DF is mainly composed of carbohydrates that are resistant to digestion and, therefore, are not absorbed by the small intestine. Thus, DF can interact directly with cells throughout the gastrointestinal tract before reaching the colon. DF can be largely metabolized by the gut microbiota in the colon, thereby reducing the size of these carbohydrates and producing short chain fatty acids (SCFA) (Tremaroli & Backhed, 2012). This SCFA release is one of the main mechanisms for the beneficial effects associated with a DF-rich diet. However, although the anticancer effects of SCFA are well known (Louis, Hold, & Flint, 2014), the mechanisms through which DF can directly interact with cancer cells is poorly understood.

Plant DF is mainly comprised of cell wall polysaccharides that are a complex network of cellulose, hemicellulose and pectin (Mohnen, 2008). Pectin is comprised of two types of polysaccharides: homogalacturonan (HG) and rhamnogalacturonan-I (RG-I). HG is composed of α−1,4-D-galacturonic acid (GalpA) residues with varying degrees of acetyl and methyl esterification (Maxwell, Belshaw, Waldron, & Morris, 2012; Mohnen, 2008), and it can be further modified by xylosylation into xylogalacturonans (XGA) or the highly complex rhamnogalacturonan-II (RG-II; Mohnen, 2008). The RG-I backbone is made of repeating units of [→4)-α-D-GalpA-(1→2)-α-L-Rha*p*-(1→] that have side groups of arabinan, galactan, and type I arabinogalactan (AGI) at the O-4 position of the rhamnose (Rha*p*) residues (Maxwell et al., 2012; Mohnen, 2008). The molecular size, monosaccharide composition, and linkage pattern of HG and RG-I vary substantially during the development of any plant species and organ, which results in a large degree of pectin heterogeneity in fruits and vegetables (Naqash, Masoodi, Ahmad Rather, Wani, & Gani, 2017). This structural diversity within a single pectin fraction makes it challenging to establish a structure-function relationship between pectin and intestinal cells.

Water-soluble citrus pectin (CP), which is mainly formed by HG (˜65%) and RG-I (˜35%), is the most studied DF from plant food sources with respect to anticancer effects (Maxwell et al., 2012). Previous studies have shown that CP exhibits no or low inhibitory effects on cancer cell proliferation and migration unless it is modified thermally, in which case stronger effects are observed (Hao et al., 2013; Jackson, Dreaden, Theobald, Tran, Beal, Eid, Stoffel et al., 2007, 2007b; Leclere, Cutsem, & Michiels, 2013, 2015; Platt & Raz, 1992). This thermal modification normally involves autoclaving CP at 121 °C for 30min to 1 h (Jackson, Dreaden, Theobald, Tran, Beal, Eid, Stoffel et al., 2007, 2007b). Modified citrus pectin (MCP) altered through this thermal process has been demonstrated to induce apoptosis of prostate cancer cells, while the effects of CP have been minimal or absent. Lung and liver cell death have also been induced by MCP (Leclere et al., 2015), as has the inhibition of colon cancer cell proliferation (Hao et al., 2013). Other studies have found that MCP inhibits cancer cell aggregation through interaction with galectin-3, where galectin-3-mediated interactions are reduced between cells and between cells and the extracellular matrix (ECM)

(Glinsky & Raz, 2009; Morris, Belshaw, Waldron, & Maxwell, 2013). The enhanced anticancer effects of CP that has been thermally modified have mostly been attributed to a reduction in molecular size, which allows the MCP to access and bind galectin-3 (Morris et al., 2013). This enhances the apoptotic activity (Jackson, Dreaden, Theobald, Tran, Beal, Eid, Stoffel et al., 2007, 2007b). While thermal modification of CP represents an inexpensive method to produce these biologically active molecules, the structural modifications and the explanation of a possible structure-function relationship still need to be elucidated. The characterization of MCP fractions will provide new insights into the relationship between the structure of MCP fragments and their effects on different cancer cells.

In the present study, thermally generated MCPs were separated into four fractions with a range of molecular size from greater than 30 kDa to less than 3 kDa. We ascertained the linkage structure of each fraction to determine the relative enrichment of HG, RG-I, and AGI. We then investigated each fraction for its anticancer properties through cell proliferation, migration and aggregation inhibitions. These different fractions have different anticancer properties, and structure- and cell- dependent effects.

2. Material and methods

2.1. Chemicals and reagents

Heat-inactivated fetal bovine serum (FBS), trypsin/EDTA and Dulbecco's modified Eagle's medium (DMEM) containing penicillin (100 UI/mL) and streptomycin (100 |Jg/mL) were from Gibco (Grand Island, NY) or Cultilab (Campinas, Brazil). Earle's Minimal Essential Medium (EMEM) was purchased from Invitrogen (Carlsbad, CA). Vybrant DiO and DiI Cell-Labeling Solution were purchased from Thermo Scientific (Waltham, MA). Antibodies for p-Akt (sc-7985-R), p-Erk (sc-7383) and Erk 1/2 (sc - 135900) were purchased from Santa Cruz Biotechnology (Santa Cruz, CA). Antibodies for Akt (#9272), p21 (2946S), PARP (#9542), cleaved caspase-3 (#9661) and p-JNK (#9255S) were purchased from Cell Signaling Technology (Beverly, MA). Rat monoclonal anti-Gal-3 antibody was obtained from the hybridoma cell line TIB-166 of the American Type Culture Collection (ATCC, Manassas, VA). Water was collected from a Milli-Q purification system from EMD Millipore (Bedford, USA). Unless stated otherwise, remaining reagents and chemicals were purchased from Sigma-Aldrich (St. Louis, USA).

2.2. Preparation of modified citrus pectin (MCP)

Pectin from citrus peel (CP; P9561 Sigma-Aldrich; ≥ 85% esterified; ≥ 74% of GalA; dextran equivalent molecular size 184.6 ± 3.1 kDa; purity 99% - ash, starch, proteins and phenolic compounds analysis) was thermally treated to produce MCP. Briefly, CP (20 g in 1.5 L in water, pH ~ 5.0, triplicate) was autoclaved (121 °C; 1 h) and MCP was recovered from solution after precipitation with cold ethanol (80% v/v final solution) overnight. MCP precipitate was extensively washed with 80% ethanol and washed twice with acetone. After acetone evaporation at 50 °C, MCP was left on a desiccator for further analysis. The MCP samples (triplicate) were water-solubilized and fractionated according to different molecular size by sequential ultrafiltration using 30, 10 and 3 kDa MWCO Amicon Ultra-4 Centrifugal

Filters (Millipore). Then, extracts were lyophilized resulting in four MCP fractions: (1) MCP higher than 30 kDa (MCP30); (2) MCP between 30 and 10 kDa (MCP30/10); (3) MCP between 10 and 3 kDa (MCP10/3); and (4) MCP lower than 3 kDa (MCP3).

2.3. Structural characterization

2.3.1. Monosaccharide analysis—MCP fractions were carboxyl-reduced with $NaBD_4$ after carbodiimide activation (Carpita & McCann, 1996; Kim & Carpita, 1992). Then, alditol acetates were prepared (Gibeaut & Carpita, 1991) and analyzed in a gaschromatography mass-spectrometry (GC-MS) system (Hewlett-Packard, Palo Alto, CA) equipped with a SP-2330 column (0.25 mm × 30 m; 0.20 μm; Supelco, Bellefonte, PA). After injection (splitless mode), the oven temperature was held at 80 °C (1 min), then increased to 170 °C at 25 °C/min, and then to 240 °C at 5 °C/min with a 10 min hold at the upper temperature. Helium was used as the carrier gas (1 mL/min). The electron impact-MS was performed at 70 eV with the temperature source at 250 °C. Pairs of diagnostic fragments *(m/z* 187/189, 217/219 and 289/291) were used to calculate the proportion of 6,6-dideuteriogalactosyl as described previously (Kim & Carpita, 1992). MCP values were achieved by all MCP fractions values corrected by their total yield in percentage.

2.3.2. Linkage analysis—MCP fractions were per-O-methylated as described previously (Gibeaut & Carpita, 1991). The same GC-MS system and column used for monosaccharide analysis were used for the analysis of partially methylated alditol acetates (PMAA). After injection (splitless mode), the oven temperature was held at 80 °C (1 min), then increased to 160 °C at 25 °C/min, to 210 °C at 2 °C/min and then to 240 °C at 5 °C/min with a 5 min hold at the upper temperature. PMAA structures were confirmed by their MS fragmentation pattern and relative retention time based on the retention time of myo-inositol (internal standard) (Kim & Carpita, 1992). MCP monosaccharide percentages were based on the relative amounts of material collected in each fraction. MCP values were achieved by all MCP fractions values corrected by their total yield in percentage.

2.3.3. Homogeneity and average molecular size—MCP and MCP fractions were analyzed by high performance size exclusion chromatography coupled to a refractive index detector (HPSEC-RID) using a 1250 Infinity system (Agilent, Santa Clara, CA) equipped with four PL-aquagel-OH columns (60, 50, 40 and 30; 300 × 7.5 mm; Agilent) connected in tandem. The eluent was 0.2 M $NaN0_3$/0.02% NaN_3 (0.6 mL/min) and the RID temperature was set at 30 °C. Dextran equivalent average molecular size was calculated using a standard curve of dextrans (MW 5–1800 kDa). The void volume (V_o) was the elution time of the heavier molecule (blue dextran; ~1800 kDa), and the elution volume (V_e) was the release time of lighter molecule (glucose).

2.3.4. Determination of the degree of O-methyl esterification—Fourier Transform Infrared (FTIR) spectroscopy was applied to determine the degree of O-methyl esterification (Manrique & Lajolo, 2002). MCP and MCP fractions were analyzed using an Alpha FTIR spectrometer (Bruker Optic, Ettlingen, Germany) equipped with a deuterated triglycine sulfate (DTGS) detector and a single bounce attenuated total reflectance (ATR) accessory (diamond crystal). FTIR-ATR spectra were obtained with a resolution of 4 cm^{-1}

and 50 scans. GRAMS/AI 9.1 software (Thermo Scientific) was used for spectra analysis. Methyl esterified and free uronic acids correspond to bands at 1749cm^{-1} and 1630 cm^{-1}, respectively, and the degree of *O*-methyl esterification was calculated using a standard curve of commercially available pectin with known degrees of O-methyl esterification (28%, 64%, 91%) and their mixtures (14%, 46%, 78%).

2.4. Cancer cell lines

HCT116 and HT29 colon and PC3 prostate cancer cell lines were purchased from ATCC and were cultured according ATCC guidelines. Briefly, cells were cultured in DMEM containing penicillin and streptomycin with 10% FBS at 37 °C in a humidified atmosphere of 5% CO_2. Cells were passed to new culture plates by using by using trypsin/EDTA when they reached 70–90% of confluence. Before treatments, cells were added to the culture plates at the desired concentration and left overnight on the incubator. After incubation, culture media was replaced by DMEM containing MCP/MCP fractions at 0.2, 0.5 or 1.0% or lactose (galetin-3 binding sugar) or sucrose (galectin-3 non-binding sugar; osmolality control) at 10, 33 or 100 mM. Cells were continuous tested for mycoplasma contamination. Cancer cells were treated with citrus pectin at a higher concentration to evaluate a cytotoxicity effect and no differences in cell proliferation were observed compared to the control (non-treated - results not shown).

2.4.1. MTT assay—Cells (1×10^4 cells/well; 96-well plate) were treated or not with MCP, MCP fractions, lactose, sucrose or 0.02% Triton X-100 (cell death control) for 24, 48, 72 and 96 h. After incubation, MTT solution in DMEM (0.5 mg/mL) was added and cells were incubated for further 3 h. Then, the supernatant was removed, formazan crystals were solubilized with DMSO and the absorbance was read at 490 nm using a Benchmark Plus Microplate Reader (Bio-Rad, Hercules, CA). Cell viability (%) was expressed in relation to the control (untreated cells).

2.4.2. LDH assay—The lactate dehydrogenase (LDH) was evaluated using the "Cytotoxicity Detection Kit" (Roche, Mannheim, Germany) following the manufacturer's instructions and accordingly to Prado et al. (2017).

2.4.3. Homotypic aggregation assay—Cells were detached from monolayer of culture plates by using 0.02% EDTA in Calcium-Magnesium free PBS (CMF-PBS) and suspended (1×10^6 cells/ mL) in CMF-PBS containing or not 20 g/mL asialofetuin and treatments. Aggregation inhibition was done accordingly to Nangia-Makker et al. (2012) and Prado et al. (2017).

2.4.4. Migration assay—Migration assay was performed as previously described (Nangia-Makker, Vitaly, & Avraham, 2012; do Prado et al., 2017). Briefly, bovine adrenal medullary endothelial cells (BAMEC) maintained in EMEM containing 10% FBS were pre-labeled with DiL (green) and incubated in one well of a 2-well culture-insert chamber (2.4×10^4 cells/well). HCT116, HT29 or PC3 cells prelabeled with DiO (red) were incubated in the other wells of the culture-insert chamber (2.4×10^4 cells/well). After 12 h, the cells were washed with PBS and the culture-insert chamber was removed. Cells were treated or not

with MCP, MCP fractions or lactose for 24 h. Migration of co-cultures toward each other was observed after 24 h using a LSM 510 META LNO Laser Scanning Microscope (Carl Zeiss, Oberkochen, Germany; The Wayne State University Microscopy and Imaging Core Facility) and migration was compared to the co-culture before treatment (0 h).

2.4.5. Wound healing assay—Wound healing assay was performed as described previously (Moreno-Bueno et al., 2009). Cancer cells were plated (2×10^5 cells/ 35-mm cell culture plate) and a wound was made by scratching the monolayer culture with a sterile micropipette tip. Then, cells were washed with PBS to remove floating cells and treated or not with MCP, MCP fractions or lactose for 24 h. Migration of cells towards gap closing was observed after 24 h using an inverted microscope (Carl Zeiss) and compared to the wound before treatment (0 h).

2.4.6. Extracellular matrix proteins (ECM) assay—ECM interaction was performed according to Nangia-Makker et al. (2012). Firstly, 96-well plates were coated with serially diluted laminin from mouse Engelbreth-Holm-Swarm (EHS) sarcoma, collagen type IV or fibronectin (10 – 0 μg) and incubated for 1 h at 37 °C. Then cell culture plates were blocked with 1% bovine serum albumin (BSA) and washed with PBS. Then, cancer cells were transferred and incubated (4.0×10^4 cells/well) in the plates containing the ECM for 16 h. Then, plates were washed to remove non-adherent cells and fluorescence levels obtained after incubation with Alamar blue (3 h) was used to define the concentration of each ECM that retained the highest number of cancer cells. After define the best concentration of each ECM (1 μg EHS laminin, 0.5 μg collagen IV and 2.5 μg fibronectin), the same experiment described above was done, but using media containing or not MCP, MCP fractions or lactose. Cells treated or not with MCP, MCP fractions or lactose were also incubated in non-coated plates (positive control) and 0.1% BSA-coated plates (negative control).

2.4.7. Apoptosis assay—Apoptosis was evaluated by flow cytometry using PE Annexin V Apoptosis Detection Kit I (BD Biosciences, San Diego, CA) according to the manufacturer's instructions. Briefly, cells (2.0×10^5 cells/well; 24-well plate) were treated or not with MCP, MCP fractions or lactose for 24 h. After incubation, cells were washed with 2% BSA in PBS and suspended in the Binding Buffer (1.0×10^6 cells /mL). Then, cell suspension (100 μL) was incubated with FITC Annexin V and 7AAD for 15min protected from light. Finally, analysis was performed using a FACSVerse flow cytometer (BD Biosciences, San Diego, CA). Controls of unstained cells and staining only with FITC Annexin V or 7AAD were used. Data analysis was performed with FlowJo software (BD Biosciences).

2.5. Western blot

Cells (5.0×10^5 cells/well; 6-well plate) were treated or not with MCP, MCP fractions or lactose and incubated for 24 h. Then, cells were washed with PBS and lysed with RIPA buffer (50 mM Tris-HCl pH 7.4, 1% NP-40, 0.5% Na-deoxycholate, 0.1% SDS, 150 mM NaCl, 2mM EDTA, 50 mM NaF and 0.2 mM Na_3VO_4) containing protease and phosphate inhibitors (Roche). Proteins were quantified using the Pierce BCA Protein Assay Kit

(Thermo Scientific). Protein separation, transfer and detection were performed accordingly to Prado et al (2017).

2.6. Hemagglutination assay inhibition with galectin-3

Recombinant galectin-3 was produced as described Nangia-Makker et al. (2012). The inhibition of hemagglutination was done as described previously (Nowak, Haywood, & Barondes, 1976; Ochieng et al., 1993). Briefly, erythrocyte was isolated from rabbit blood and a final suspension of 4% was used in experiment. In each well of a V plate was add 50 μL of 1% bovine serum albumin (BSA), 50 μL of PBS 1× or the sample diluted in PBS 1× and/or 10 μg/mL galectin-3, and 25 μL of rabbit erythrocyte. After, the plate was incubated on room temperature for 90 min.

2.7. Statistical analysis

The results were expressed as the mean ± standard deviation (SD) and the images were representative of at least three independent experiments, except for WB analysis, which were performed in duplicate. Data were analyzed using GraphPad Prism 6.0 software (GraphPad Software, San Diego, CA). One-way ANOVA with Tukey's (to assess differences between all groups) or Dunnett's (to assess differences between the control and two or more groups) were used as post hoc tests, and Least Significant Difference (LSD) was used to compare means at 0.0001. Significance was set at $p < 0.05$.

3. Results and discussion

3.1. Thermal modification leads to structural differences among MCP fractions

The yield of MCP fractions was based on the total MCP that was separated. The MCP30 fraction was the most abundant (68 ± 1% w/ w), followed by MCP 30/10 (15 ± 1% w/w), MCP10/3 (10 ± 0% w/ w), and MCP3 (7 ± 0% w/w). HPSEC-RID confirmed sequential ultrafiltration of the separated MCP fractions according to their molecular size (Table 1). The dextran equivalent average molecular sizes were calculated using three replicates of MCP30, MCP30/10, MCP10/3 and MCP3 fractions and the results of the main peaks were 35.2 kDa, 27.5 kDa, 10.2 kDa, and 5.1 kDa, respectively (Table 1). We also calculated the maximum and minimum values at half height for each analysis (Supplemental Figure S1).

Monosaccharide analysis showed that galacturonic acid GalA was the most abundant monosaccharide in all the MCP fractions, followed by galactose (Gal; Table 1). Among the MCP fractions, MCP10/3had the highest level of Gal and the lowest level of GalA. Degrees of es- terification were similar for fractions of larger molecular size, ranging from 79 to 85%, whereas degree of esterification was 54% in MCP3 (Table 1). Linkage analysis showed that the most prevalent form of GalA in all the fractions was 4-GalA (Fig. 1; Supplemental Table S1), indicating that all MCP was mostly HG. The presence of a small amount of *3,4*-GalA and the corresponding *t*-Xyl residues demonstrated that XGA was also part of the HG fraction. Smaller amounts of *2*-Rha, *2,4*-Rha and an equal amount of *4*-GalA indicated the presence of RG-I. The *4*-Gal and *3,4*-Gal, and a corresponding amount of *t*-Ara*f* equal to the branch points were taken as evidence for the presence of AGI. Similar results between the monosaccharide composition and linkage patterns of MCP, MCP30 and

MCP30/10 were found. Notably, MCP10/3 and MCP3 showed a strong decrease in GalA : *t*-GalA, consistent with a decreased molecular size (Supplemental Table S2). MCP10/3had higher proportions of *4*-Gal, *3,4*-Gal, and the corresponding *t*-Araf, as well as enrichment of Gal, indicating higher amounts of AGI compared to the other MCP fractions. When some linkages were gathered into the probable polysaccharide structures, HG (*4*-GalA and *t*-GalA) fragments become the dominant ones with a decrease in MCP10/3 due to AGI increase (*4*-Gal, *3,4*-Gal, *4,6*-Gal and *t*-Araf). Minor changes between MCP fractions were observed for: RG-I (*2*-Rha, *2,4*-Rha, *3,4*-GalA and *4*-GalA), type II arabinogalactan (AGII - *3*-Gal, *6*-Gal, *2*-Ara, *3,6*-Gal, *3,4,6*-Gal, *t*-Rha, *t*-Ara), heteroxylan (e.g. glucuronoarabinoxylan; *4*-Xyl, *2,4*-Xyl, *3,4*-Xyl, *2,3,4*-Xyl, *t*-GlcA, *t*-Ara), heteromannan (e.g. glucomannan; *4*-Man, *4,6*-Man, *4*-Glc, *4,6*-Glc, *t*-Gal), arabinan (*5*-Ara, *2,5*-Ara, *3,5*-Ara, *t*-Ara) and xyloglucan (*4,6*-Glc, *4*-Glc, *2*-Xyl, *2*-Gal, *t*-Fuc, *t*-Xyl). Others partially methylated alditol acetate residues did not change between MCP fractions (*t*-Ara*p*, *3*-Araf, Ara(OAc)5, Xyl(OAc)5, Man(OAc)6, *2,4*-Gal, *2,4,6*-Gal, Gal(OAc)6, *4,6*-GalA, *2,4*-GalA, *3,4*-Glc, Glc(OAc)6) (Pettolino, Walsh, Fincher, & Bacic, 2012).

MCP, MCP30 and MCP30/10 are mainly composed of highly esterified HG and similar proportions of RG-I and AGI. The MCP10/3 fraction was also characterized by highly esterified HG, but with higher quantities of AGI, while MCP3 had fewer branched structures (RG-I and AGI) with lesser degree of esterification and a smaller molecular size. The characteristics of smaller but high-methylated MCP10/3 fraction and the smaller but low-methylated MCP3 fraction may result in differences in biological effects (Chen et al., 2006). MCP10/3 fraction possesses promising biologically active structures since methylated structures, the HG:RG-I ratio and the higher AGI quantity are requisites in enhancing the anticancer effects (Maxwell et al., 2016).

3.2. MCP fractions differentially regulate cancer cells proliferation, migration, and aggregation

Three cell lines were used to observe how different cancer cell mutations responded to treatment with MCP fractions with respect to necrosis, necroptosis, apoptosis, viability, and cytotoxicity. HCT116 and HT29 are colon cancer cell lines, while PC3 is a prostate cancer cell line. Initial screening was made to investigate the effects of MCP and MCP fractions on cell viability using sucrose, lactose and CP as controls (Supplemental Figure S2). Viability was measured by 3-(4,5-Dimethyl-2-thiazolyl)-2,5-diphenyl-2H-tetrazolium bromide (MTT) and sucrose and lactose were used as a control of galectin-3 non-binding and ga- lectin-3 binding carbohydrates, respectively (Barondes, Cooper, Gitt, & Leffler, 1994). The screening for a loss in cancer cell viability (compared with a control without treatment) showed that after a 24 h-in-cubation with sucrose and lactose at 100 mM, a loss of cancer cell viability was observed (Supplemental Figure S2). No loss in cell viability was seen with a treatment of CP. Lactose at 100 mM is widely used for galectin-3 inhibition since it is non-cytotoxic (Inohara & Raz, 1995; Mina-Osorio, Soto-Cruz, & Ortega, 2007). In the same manner as the simpler carbohydrates, cells treated with MCP and MCP fractions at 1.0% also exhibited reduced cell viability (Fig. 2).

Thus, for comparison experiments, a 24 h-incubation period was used with 1.0% MCP and MCP fractions and 100 mM of lactose and sucrose. To determine if the reduction in cell viability was a result of cytotoxicity, the lactate dehydrogenase (LDH) assay was performed. Results showed that a significant cytotoxicity was observed only for HCT116 cells after treatment with MCP10/3 (Fig. 3), highlighting that MCP fractions may have distinct effects in different cancer cells with respect to cell death, but these mechanisms need to be further investigated.

Annexin V is a protein that binds to the negative heads of phosphatidylserine in the external monolayer of the membrane. When this protein is conjugated with a fluorochrome, the cellular fraction that increases the translocation of negative phospholipids to the outer monolayer of the membrane can be determined. The fluorescent DNA marker 7-AAD intercalates within DNA, and it requires a prior permeabilization of the plasma membrane. The translocation of phospholipids in the outer monolayer of the membrane is considered an early event in the triggering of cell death by apoptosis (quadrant Q1). The permeabilization of the membrane only occurs during necrotic processes (quadrant Q3), and when both events happen it could be indicative of late apoptosis/necroptosis (quadrant Q2). The MCP30/10 and MCP10/3 fractions induced necrosis (Q1) and necroptosis (Q2) in HCT116 and PC3 cells but not in HT29 cells (Fig. 4; Supplemental Figure S3). It has been suggested that MCP30/10 and MCP10/3have the same esterification degree and the lowest molecular size of the other fractions except for MCP3.

These chemical and structural differences could explain why MCP30/10 and MCP10/3 increased necroptosis in HCT116 cells while MCP3 did not, since the higher the degree of esterification the better the programmed cell death activation on cancer cells (Jackson, Dreaden, Theobald, Tran, Beal, Eid, Stoffel et al., 2007, 2007b).

Because the size and number of cancer cell aggregates have been found to correlate with cell survival (Zhang, Lu, Dazin, & Kapila, 2004) and because cancer cells that form aggregates in suspension cultures have been found to exhibit significantly lower levels of death than single cells (Zhang, Xu, & Yu, 2010), MCP and MCP fractions were evaluated for the inhibition of cancer cell aggregation. In the aggregation assay, asialofetuin was used to induce cell aggregation, and lactose, which inhibits lectins-dependent aggregation, was used as a positive control. The inhibition of aggregation induced by MCP3 was similar to lactose in all three cell lines (Fig. 5). Similar effects compared to lactose were also found for MCP30/10 and MCP10/3 in HT29 cells (Supplemental Figure S4).

Cell migration and attachment to the ECM are crucial steps to cancer development and metastasis. Thus, the effects of MCP and MCP fractions on cancer cell migration towards endothelial cells and cell attachment to proteins of the ECM were evaluated by migration assay. MCP3 strongly inhibited cancer cell migration in all three cell lines, but the effects were strongest for HCT116 cells (Fig. 6). MCP30/10 and MCP10/3 also strongly inhibited migration of HCT116 cells, but MCP and MCP30 did not. The inhibitory effects of MCP3 as well as the absence of effects for both MCP and MCP30 on cancer cell migration were confirmed by the wound healing assay (Supplemental Figure S5).

MCP3 gap closing was 27.5 ± 0.3% compared to 63.5 ± 0.7% for the control for HCT116, 14.5 ± 0.3% compared to 22.6 ± 1.3% for the control for HT29, and 51.6 ± 4.2% compared to 77.4 ± 3.8% for the control (Supplemental Figure S5).

The ECM-protein assay evaluated the effects of MCP and MCP fractions on inhibiting the interactions between cancer cells and several target ECM proteins (laminin, collagen IV, and fibronectin). Polysaccharides that are chemically similar to some glycoproteins could interfere with cancer cell adhesion to ECM proteins and the inhibition of galectin-3. ECM proteins, such as laminin, collagen IV, and fibronectin are required for cancer cell growth and invasion as previously shown (Pickup, Mouw, & Weaver, 2014). As lactose inhibits lectin-dependent interaction between cells and ECM proteins, it was used as a positive control. MCP10/3 and MCP3 reduced HCT116, HT29, and PC3 cell density in laminin-coated plates, reduced HCT116 cell density in collagen IV-coated plates, and also reduced HT29 cell density in fibronectin-coated plates (Fig. 7). In contrast, MCP30/10 only reduced HT29 and HCT116 cell density in laminin-coated plates, whereas MCP30 had a similar effect to that of lactose only in PC3 cell density in laminin-coated plates. The interference of MCP fractions on the adhesion of cancer cells to ECM proteins may be representative of a positive effect against cancer cell spread and metastasis, opening new avenues for the identification of bioactive carbohydrates derived from fruit.

The effects of MCP and MCP fractions on the protein levels normally associated with cancer cell death, survival, and migration were evaluated to yield clues on the biochemical mechanisms of why cancer cells are affected by these treatments. While pAKT (phosphorylated protein kinase B) is normally related to cell survival (Brunet et al., 1999), higher concentrations cause excessive cell stress leading to necroptosis (Buchheit, Rayavarapu, & Schafer, 2012; Zhao et al., 2017). Increased pERK levels are normally linked to cell migration and survival (Han, Khuri, & Roman, 2006; More, Chiplunkar, & Kalraiya, 2016; Xue & Hemmings, 2013), but pERK up-regulation can also induce cell necrosis by necroptosis or autophagy (He et al., 2013). Protein p21 can cause cell cycle arrest and cell death (Masgras et al., 2012), and PARP has a role in DNA repair and promotion of cell survival (D'Arcangelo, Drew, & Plummer, 2011). Caspase-3 plays an important role in apoptosis (Nicholson, 1999), and pJNK can be involved in cancer cell growth, survival, and metastasis (Dhanasekaran, 2013). Immuno-gel blot analysis demonstrated that the MCP and MCP fractions differentially regulated the expression of these proteins in cancer cells (Fig. 8; Supplemental Figure S6). MCP and MCP30 reduced pAKT levels in HCT116, HT29, and PC3 cells; however, only MCP increased pERK1/2 and p21 levels in HCT116 and PC3 cells, respectively. MCP30/10 increased pAKT and p21 levels in HCT116 and PC3 cells, whereas MCP10/3 increased only p21 levels, but not those of pAKT. The MCP3 fraction had differential effects on protein levels in HCT116, HT29, and PC3 cell lines; this fraction increased p21 levels and induced caspase-3 expression in HCT116 cells, but reduced pERK levels in HT29 cells. MCP3 enhanced p21 expression and reduced pJNK levels in HT29 and PC3 cells, but PARP and Galectin-3 levels did not change throughout the treatments.

It seems that higher AGI levels and lower RG-I levels are required to activate p21, as MCP30/10, MCP10/3, and MCP3 treatments increased this protein level in HCT116, with an activation of p21 being related to cell cycle arrest that induces cell death (Masgras et al.,

2012). Apoptosis in MCP3 treatment in HCT116 could be triggered by caspase-3 activation, but the higher levels of p21 and the lowest quantity of dead cells when compared to MCP30/10 and MCP10/3 are indicators that other biochemical pathways that lead to cell death might have been activated or repressed. MCP10/3 promoted the reduction of pAKT levels in HCT116, and since increased levels of pAKT are normally related to cell survival (Brunet et al., 1999), this could explain the reduction in cell proliferation and the inhibitory effects on cell migration that were observed. On the other hand, the MCP30/10 induced pAKT expression in PC3 cells could have led to the observed cell proliferation reduction and cell migration inhibition. This could be due to the higher HG fractions in MCP30/10. Since MCP30/10has the lesser amount of *t*-GalA of all the fractions, it is possible to speculate that HG is important for pAKT expression and/or AKT phosphorylation and could cause an excessive stress to cells leading to necroptosis (Buchheit, Rayavarapu, & Schafer, 2012; Zhao et al., 2017). Our results demonstrate that the smaller MCP fractions (MCP30/10, MCP10/3, and MCP3) were more effective in reducing cancer cell proliferation, migration, and adhesion to ECM proteins. All MCP fractions showed some biological effects in at least one of the three cell lines tested. Thus, the underlying mechanisms of MCP fractions in cancer cells seem to be both structure- and cell line-dependent. The three cell lines used have different characteristics. HT29 is a colon adenocarcinoma cell line, while HCT116 is a colon carcinoma cell line. HT29 cells are differentiated, while HCT116 cells are poorly differentiated and highly metastatic. And PC3 is a highly metastatic adenocarcinoma cell line (American Type Culture Collection, 2013; Tai et al., 2011).

3.3. Galectin-3 inhibition is dependent on MCP structure rather than molecular size

Galectin-3 is a member of the carbohydrate-binding protein family that exhibits an affinity for β-galactoside sugars in a conserved sequence of the carbohydrate-binding site (Barondes et al., 1994). The overexpression of galectin-3 might induce cancer cells to become more aggressive by increasing their proliferation and metastasis (Dumic, Dabelic, & Flogel, 2006). Therefore, the interaction of pectin fractions with galectin-3 could prevent this increased activity in cancer cells. Because at least part of the anticancer effects of MCP were related to the inhibition of galectin-3, the hemagglutination assay was performed to evaluate the possible interaction between MCP fractions and galectin-3. High concentrations of CP (negative control) did not inhibit galectin-3-mediated hemagglutination (Supplemental Figure S7). In contrast, MCP and MCP30 inhibited galectin-3-mediated hemagglutination at 400 μg/ mL. Notably, MCP30/10 did not inhibit galectin-3-mediated hemagglutination even at higher concentrations (500 μg/mL), and MCP10/3 and MCP3had inhibitory effects at lower concentrations (300 μg/mL). As all fractions possessed high amounts of GalA, the greater activity of the smaller fractions in binding to galectin-3 may explain why the minimum inhibitory concentration was much higher than that of lactose. Gao et al. (2012) fractioned a chemically MCP and demonstrated that neutral fractions showed less galectin-3 binding than did acidic fractions. In our study, thermally MCP fractionated by size showed different galectin-3 binding powers, with the smaller sizes resulting in more inhibition, probably enhancing the observed anticancer activity due to a better penetration in cancer cells because of their smaller molecular sizes.

A concern about thermally modified pectin is the production of cytotoxic molecules and β-elimination with a consequent production of unsaturated sugar residues (Leclere et al., 2016; Zhang, Xu, & Zhang, (2015). Using the same HPLC-UV protocol described in Leclere et al. (2016), we did not find any cyclic compounds in our thermally MCP or in the fractionated samples (data not shown). One explanation for not detecting the low molecular size compounds produced by Maillard reactions, differing from the results of Leclere et al. (2016), is that we precipitated our pectin with ethanol and exhaustively washed the precipitate with 80% ethanol and with acetone. This protocol might have removed any cytotoxic compounds. Moreover, the measurement of UV absorbance (from 210 nm to 260 nm) did not reveal any conjugated dienes produced by β-elimination, possibly because the pH had not been adjusted to 7.0 prior to the heat treatment. Another consequence of β-elimination would be a reduced esterification of the HG backbone, which was not observed in our samples despite the smaller one (with low quantity also). Therefore, the effects observed in our study did not seem to be related to the cytotoxic molecules reported elsewhere (Leclere et al., 2016).

4. Conclusions

This study demonstrates that treatment with MCP fractions that are fractionated by molecular size results in diverse effects on cancer cell proliferation, migration, and aggregation. These effects were size-, structure-, and cell line-dependent. Beside the smaller sizes, the enrichment of AGI in MCP10/3 and MCP3 with fewer branched structures (RG-I and AGI) and more de-esterified HG oligomers enhances anticancer effects by inhibiting cancer cell migration, aggregation, and proliferation. Furthermore, MCP fractions differentially interact with ECM proteins and galectin-3. Thus, MCP fractionation is an important tool to define possible structure-function relationships. Furthermore, we predict that MCP fractionation will be useful in the development of functional MCP-derived products and food supplements.

Supplementary Material

Refer to Web version on PubMed Central for supplementary material.

Acknowledgements

Authors thank Dhong Hyo Kho and Pratima Nangia-Makker for their valuable scientific instructions and discussion. This research was financially supported by grants #2012/23970-2 and #2013/07914-8, São Paulo Research Foundation (FAPESP). A multiuser equipment was used (#2015/01004-5, São Paulo Research Foundation (FAPESP)). Scholarships were awarded to SBRP by the National Council for Scientific and Technological Development (CNPq; 167934/2014-7) and to TMS (CAPES Process BEX-10734/13-9).

References

American Type Culture Collection (2013). Colon cancer and normal cell lines. ATCC Retrieved from http://www.atcc.org/~/media/PDFs/CancerandNormalcelllinestables/Coloncancerandnormalcelllines.ashx.

Barondes SH, Cooper DNW, Gitt MA, & Leffler H (1994). Galectins: Structure and function of a large family of animal lectins. Journal of Biological Chemistry, 269(33), 20807–20810. 10.1016/j.celrep.2015.02.012. [PubMed: 8063692]

Brunet A, Bonni A, Zigmond MJ, Lin MZ, Juo P, Hu LS, ... Greenberg ME (1999). Akt promotes cell survival by phosphorylating and inhibiting a forkhead transcription factor. Cell, 96(6), 857–868. 10.1016/S0092-8674(00)80595-4. [PubMed: 10102273]

Buchheit CL, Rayavarapu RR, & Schafer ZT (2012a). The regulation of cancer cell death and metabolism by extracellular matrix attachment. Seminars in Cell & Developmental Biology, 23(1096–3634 (Electronic)), 402–411. 10.1016/j.semcdb.2012.04.007. [PubMed: 22579674]

Buchheit CL, Rayavarapu RR, & Schafer ZT (2012b). The regulation of cancer cell death and metabolism by extracellular matrix attachment. Seminars in Cell & Developmental Biology, 23(1096–3634 (Electronic)), 402–411. 10.1016/j.semcdb.2012.04.007. [PubMed: 22579674]

Carpita NC, & McCann MC (1996). Some new methods to study plant polyuronic acids and their esters In Townsend R, & Hotchkiss A (Eds.). Progress in glycobiology (pp. 595–661). New York, NY: Marcel Dekker.

Chen CH, Sheu MT, Chen TF, Wang YC, Hou WC, Liu DZ, ... Liang YC (2006). Suppression of endotoxin-induced proinflammatory responses by citrus pectin through blocking LPS signaling pathways. Biochemical Pharmacology, 72(8), 1001–1009. 10.1016/j.bcp.2006.07.001. [PubMed: 16930561]

D'Arcangelo M, Drew Y, & Plummer R (2011). The role of PARP in DNA repair and its therapeutic exploitation. British Journal of Cancer, 105, 1114–1122. 10.1016/B978-0-12-803582-5.00004-8. [PubMed: 21989215]

Dhanasekaran DN (2013). JNK signaling network and cancer. Genes & Cancer, 4(9–10), 332–333. 10.1177/1947601913507949. [PubMed: 24349630]

do Prado SBR, Ferreira GF, Harazono Y, Shiga TM, Raz A, Carpita NC, et al. (2017). Ripening-induced chemical modifications of papaya pectin inhibit cancer cell proliferation. Sci Rep. 7, 16564 10.1038/s41598-017-16709-3. [PubMed: 29185464]

Dumic J, Dabelic S, & Flogel M (2006). Galectin-3: An open-ended story. Biochimica et Biophysica Acta, 1760(4), 616–635. 10.1016/j.bbagen.2005.12.020. [PubMed: 16478649]

Gao X, Zhi Y, Zhang T, Xue H, Wang X, Foday AD, ... Zhou Y (2012). Analysis of the neutral polysaccharide fraction of MCP and its inhibitory activity on galectin-3. Glycoconjugate Journal, 29(4), 159–165. 10.1007/s10719-012-9382-5. [PubMed: 22562786]

Gibeaut DM, & Carpita NC (1991). Clean-up procedure for partially methylated alditol acetate derivatives of polysaccharides. Journal of Chromatography, 587, 284–287 https://doi.org/0021-9673/91.

Glinsky VV, & Raz A (2009). Modified citrus pectin anti-metastatic properties: One bullet, multiple targets. Carbohydrate Research, 344(14), 1788–1791. 10.1016/j.carres.2008.08.038. [PubMed: 19061992]

Han S, Khuri FR, & Roman J (2006). Fibronectin stimulates non-small cell lung carcinoma cell growth through activation of Akt/mammalian target of rapamycin/S6 kinase and inactivation of LKB1/AMP-activated protein kinase signal pathways. Cancer Research, 66(1), 315–323. 10.1158/0008-5472.CAN-05-2367. [PubMed: 16397245]

Hao M, Yuan X, Cheng H, Xue H, Zhang T, Zhou Y, ... Tai G (2013). Comparative studies on the anti-tumor activities of high temperature- and pH-modified citrus pectins. Food & Function, 4(6), 960–971. 10.1039/c3fo30350k. [PubMed: 23673419]

He W, Wang Q, Srinivasan B, Xu J, Padilla MT, Li Z, ... Lin Y (2013). A JNK-mediated autophagy pathway that triggers c-IAP degradation and necroptosis for anticancer chemotherapy. Oncogene, 33(23), 3004–3013. Retrieved from http://www.ncbi.nlm.nih.gov/pubmed/23831571. [PubMed: 23831571]

Inohara H, & Raz A (1995). Functional evidence that cell surface galectin-3 mediates homotypic cell adhesion. Cancer Research, 55(15), 3267–3271. [PubMed: 7542167]

Jackson CL, Dreaden TM, Theobald LK, Tran NM, Beal TL, Eid M, ... Mohnen D (2007). Pectin induces apoptosis in human prostate cancer cells: Correlation of apoptotic function with pectin structure. Glycobiology, 17(8), 805–819. 10.1093/glycob/cwm054. [PubMed: 17513886]

Jackson CL, Dreaden TM, Theobald K, Tran NM, Beal TL, Eid M, ... Stoffel T (2007). Pectin induces apoptosis in human prostate cancer cells: Correlation of apoptotic function with pectin structure. Glycobiology, 17(8), 805–819. 10.1093/glycob/cwm054. [PubMed: 17513886]

Kim JB, & Carpita NC (1992). Changes in esterification of the uronic acid groups of cell wall polysaccharides during elongation of maize coleoptiles. Plant Physiology, 98(2), 646–653. 10.1104/pp.98.2.646. [PubMed: 16668690]

Leclere L, Cutsem PV, & Michiels C (2013). Anti-cancer activities of pH- or heat-modified pectin. Frontiers in Pharmacology, 4, 128 10.3389/fphar.2013.00128. [PubMed: 24115933]

Leclere L, Fransolet M, Cambier P, El Bkassiny S, Tikad A, Dieu M, ... Michiels C (2016). Identification of a cytotoxic molecule in heat-modified citrus pectin. Carbohydrate Polymers, 137, 39–51. 10.1016/j.carbpol.2015.10.055. [PubMed: 26686103]

Leclere L, Fransolet M, Cote F, Cambier P, Arnould T, Van Cutsem P, ... Michiels C (2015). Heat-modified citrus pectin induces apoptosis-like cell death and autophagy in HepG2 and A549 cancer cells. PloS One, 10(3), e0115831. 10.1371/journal.pone.0115831.

Louis P, Hold GL, & Flint HJ (2014). The gut microbiota, bacterial metabolites and colorectal cancer. Nature Reviews Microbiology, 12(10), 661–672. 10.1038/nrmicro3344. [PubMed: 25198138]

Manrique GD, & Lajolo FM (2002). FT-IR spectroscopy as a tool for measuring degree of methyl esterification in pectins isolated from ripening papaya fruit. Postharvest Biology and Technology, 25(1), 99–107. 10.1016/S0925-5214(01)00160-0.

Masgras I, Carrera S, De Verdier PJ, Brennan P, Majid A, Makhtar W, ... Macip S (2012). Reactive oxygen species and mitochondrial sensitivity to oxidative stress determine induction of cancer cell death by p21. Journal of Biological Chemistry, 287(13), 9845–9854. 10.1074/jbc.M111.250357. [PubMed: 22311974]

Maxwell EG, Belshaw NJ, Waldron KW, & Morris VJ (2012). Pectin - An emerging new bioactive food polysaccharide. Trends in Food Science & Technology, 24(2), 64–73. 10.1016/j.tifs.2011.11.002.

Maxwell EG, Colquhoun IJ, Chau HK, Hotchkiss AT, Waldron KW, Morris VJ, ... Belshaw NJ (2016). Modified sugar beet pectin induces apoptosis of colon cancer cells via an interaction with the neutral sugar side-chains. Carbohydrate Polymers, 136, 923–929. 10.1016/j.carbpol.2015.09.063. [PubMed: 26572430]

Mina-Osorio P, Soto-Cruz I, & Ortega E (2007). A role for galectin-3 in CD13-mediated homotypic aggregation of monocytes. Biochemical and Biophysical Research Communications, 353(3), 605–610. 10.1016/j.bbrc.2006.12.081. [PubMed: 17189612]

Mohnen D (2008). Pectin structure and biosynthesis. Current Opinion in Plant Biology, 11(3), 266–277. 10.1016/j.pbi.2008.03.006. [PubMed: 18486536]

More SK, Chiplunkar SV, & Kalraiya RD (2016). Galectin-3-induced cell spreading and motility relies on distinct signaling mechanisms compared to fibronectin. Molecular and Cellular Biochemistry, 416(1–2), 179–191. 10.1007/s11010-016-2706-1. [PubMed: 27130204]

Moreno-Bueno G, Peinado H, Molina P, Olmeda D, Cubillo E, Santos V, ... Cano A (2009). The morphological and molecular features of the epithelial-to-mesenchymal transition. Nature Protocols, 4(11), 1591–1613. 10.1038/nprot.2009.152. [PubMed: 19834475]

Morris VJ, Belshaw NJ, Waldron KW, & Maxwell EG (2013). The bioactivity of modified pectin fragments. Bioactive Carbohydrates and Dietary Fibre, 1(1), 21–37. 10.1016/j.bcdf.2013.02.001.

Nangia-Makker P, Vitaly B, & Avraham R (2012). Galectin-3-binding and metastasis. Methods in Molecular Biology, 878(18), 241–250. 10.1007/978-1-61779-854-2. [PubMed: 22674138]

Naqash F, Masoodi FA, Ahmad Rather S, Wani SM, & Gani A (2017). Emerging concepts in the nutraceutical and functional properties of pectin - a review. Carbohydrate Polymers, 168, 227–239. 10.1016/j.carbpol.2017.03.058. [PubMed: 28457445]

Nicholson D (1999). Caspase structure, proteolytic substrates and function during apoptotic cell death. Cell Death & Differentiation, 6(11), 1028–1042. 10.1038/sj.cdd.4400598. [PubMed: 10578171]

Nowak TP, Haywood PL, & Barondes SH (1976). Developmentally regulated lectin in embryonic chick muscle and a myogenic cell line. Biochemical and Biophysical Research Communications, 68(3), 650–657. [PubMed: 1259723]

O'Keefe SJD (2016). Diet, microorganisms and their metabolites, and colon cancer. Nature Reviews Gastroenterology and Hepatology, 13(12), 691–706. 10.1038/nrgastro.2016.165. [PubMed: 27848961]

Ochieng J, Platt D, Tait L, Hogan V, Raz T, Carmi P, ... Raz A (1993). Structure-function relationship of a recombinant human galactoside-binding protein. Biochemistry, 32(16), 4455–4460. Retrieved from http://www.ncbi.nlm.nih.gov/pubmed/8476870. [PubMed: 8476870]

Pettolino F, Walsh C, Fincher GB, & Bacic A (2012). Determining the polysaccharide composition of plant cell walls. Nature Protocols, 7(9), 1590–1607. 10.1038/nprot.2012.081. [PubMed: 22864200]

Pickup MW, Mouw JK, & Weaver VM (2014). The extracellular matrix modulates the hallmarks of cancer. EMBO Report, 15(12), 1243–1253. 10.15252/embr.201439246.

Platt D, & Raz A (1992). Modulation of the lung colonization of b16-f1 melanoma cells by citrus pectin. Journal of the National Cancer Institute, 84, 438–442. [PubMed: 1538421]

Tai S, Sun Y, Squires JM, Zhang H, Oh WK, Liang CZ, ... Huang J (2011). PC3 is a cell line characteristic of prostatic small cell carcinoma. Prostate, 71(15), 1668–1679. 10.1002/pros.21383. [PubMed: 21432867]

Tremaroli V, & Backhed F (2012). Functional interactions between the gut microbiota and host metabolism. Nature, 489(7415), 242–249. 10.1038/nature11552. [PubMed: 22972297]

Vieira AR, Abar L, Chan DSM, Vingeliene S, Polemiti E, Stevens C, ... Norat T (2017). Foods and beverages and colorectal cancer risk: A systematic review and meta-analysis of cohort studies, an update of the evidence of the WCRF-AICR Continuous Update Project. Annals of Oncology, 28(8), 1788–1802. 10.1093/annonc/mdx171. [PubMed: 28407090]

Xue G, & Hemmings BA (2013). PKB/akt-dependent regulation of cell motility. Journal of the National Cancer Institute, 105(6), 393–404. 10.1093/jnci/djs648. [PubMed: 23355761]

Zhang W, Xu P, & Zhang H (2015). Pectin in cancer therapy: A review. Trends in Food Science & Technology, 44(2), 258–271. 10.1016/j.tifs.2015.04.001.

Zhang X, Xu LH, & Yu Q (2010). Cell aggregation induces phosphorylation of PECAM-1 and Pyk2 and promotes tumor cell anchorage-independent growth. Molecular Cancer, 9, 1–11. 10.1186/1476-4598-9-7. [PubMed: 20051109]

Zhang Y, Lu H, Dazin P, & Kapila Y (2004). Squamous cell carcinoma cell aggregates escape suspension-induced, p53-mediated anoikis: Fibronectin and integrin αv mediate survival signals through focal adhesion kinase. Journal of Biological Chemistry, 279(46), 48342–48349. 10.1074/jbc.M407953200. [PubMed: 15331608]

Zhao Y, Hu X, Liu Y, Dong S, Wen Z, He W, ... Huang Q (2017). ROS signaling under metabolic stress: Cross-talk between AMPK and AKT pathway. Molecular Cancer, 16(1), 79 10.1186/s12943-017-0648-1. [PubMed: 28407774]

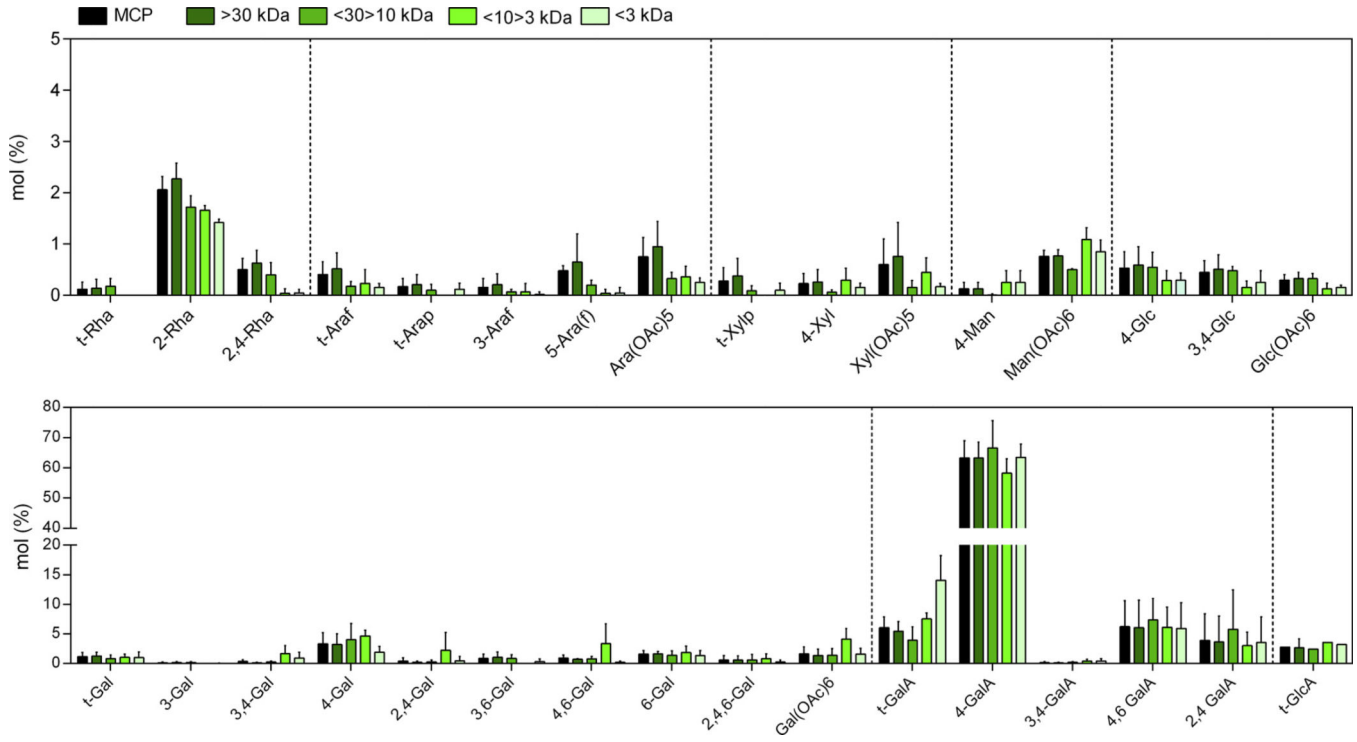

Fig. 1.

Linkage analysis of MCP and MCP fractions. The table of linkage results is presented in Supplemental Table 1. Rhamnose (Rha); fucose (Fuc); arabinose (Ara); xylose (Xyl); mannose (Man); galactose (Gal); Galacturonic acid (GalA); glucose (Glc); glucuronic acid (GlcA); terminal (t); pyranose (p); furanose (f). MCP: modified citrus pectin.

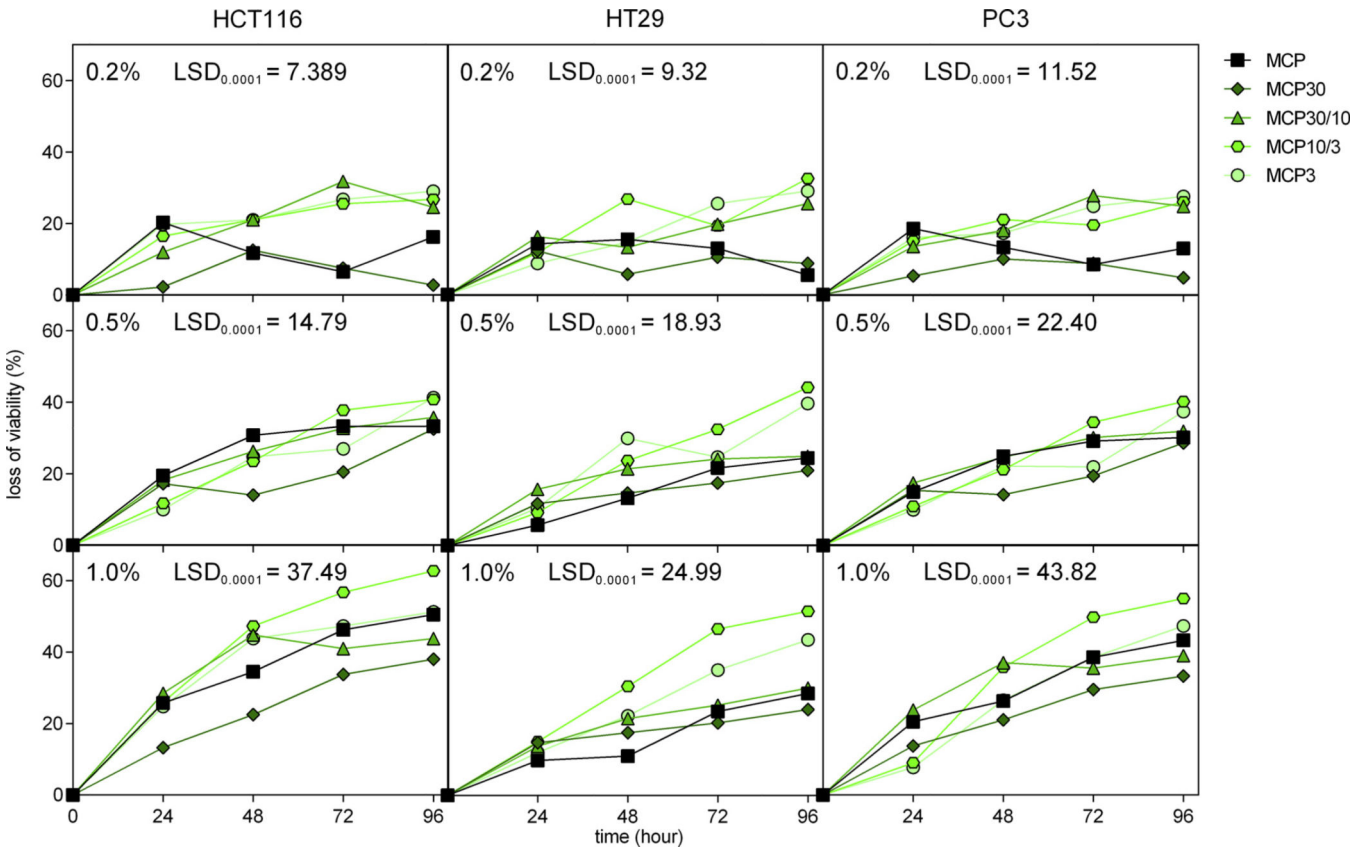

Fig. 2.

Cell viability loss after MCP and MCP fractions treatment. The loss of viability was calculated based on control (without treatment) as 100%. Cells were treated with MCP and MCP fractions at different concentrations (0.2%, 0.5% and 1%) and the higher concentrations and the lower fractions precluded cells growth. Data were shown as mean values. One-way ANOVA with the Least Significant Difference (LSD) test was used to compare means at 0.0001. Significant mean values are those with differences larger than the LSD value showed in each graphic. The results were from three independent experiments, with each performed in triplicate. The complete data are presented in Table S3.

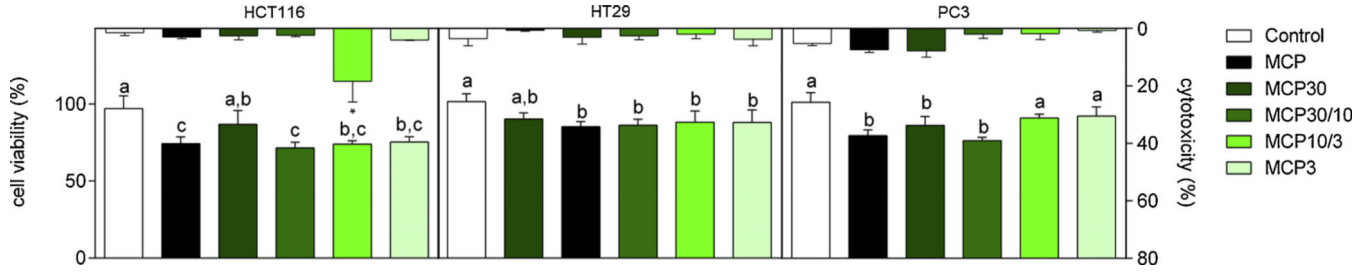

Fig. 3.

Cell viability by MTT assay (left x axis) and cells cytotoxicity after 24 h of treatment by LDH assay (right x axis). Effects on cell viability of the higher concentration of MCP and MCP fractions (1%) at t = 24 h are shown on lower graphic. Data are shown as mean ± SD. Tukey's test (*$p < 0.05$) was performed. Different letters represent significant differences between the treatments. Cytotoxicity by LDH assay after 24 h of incubation is shown in upper graphic. Data are expressed as percentage of cell viability compared to control (no treatment) of each time. Results are represented as mean ± SD of three independent experiments, with each performed in triplicate. *$p < 0.05$ vs control, according to Dunnetts's test.

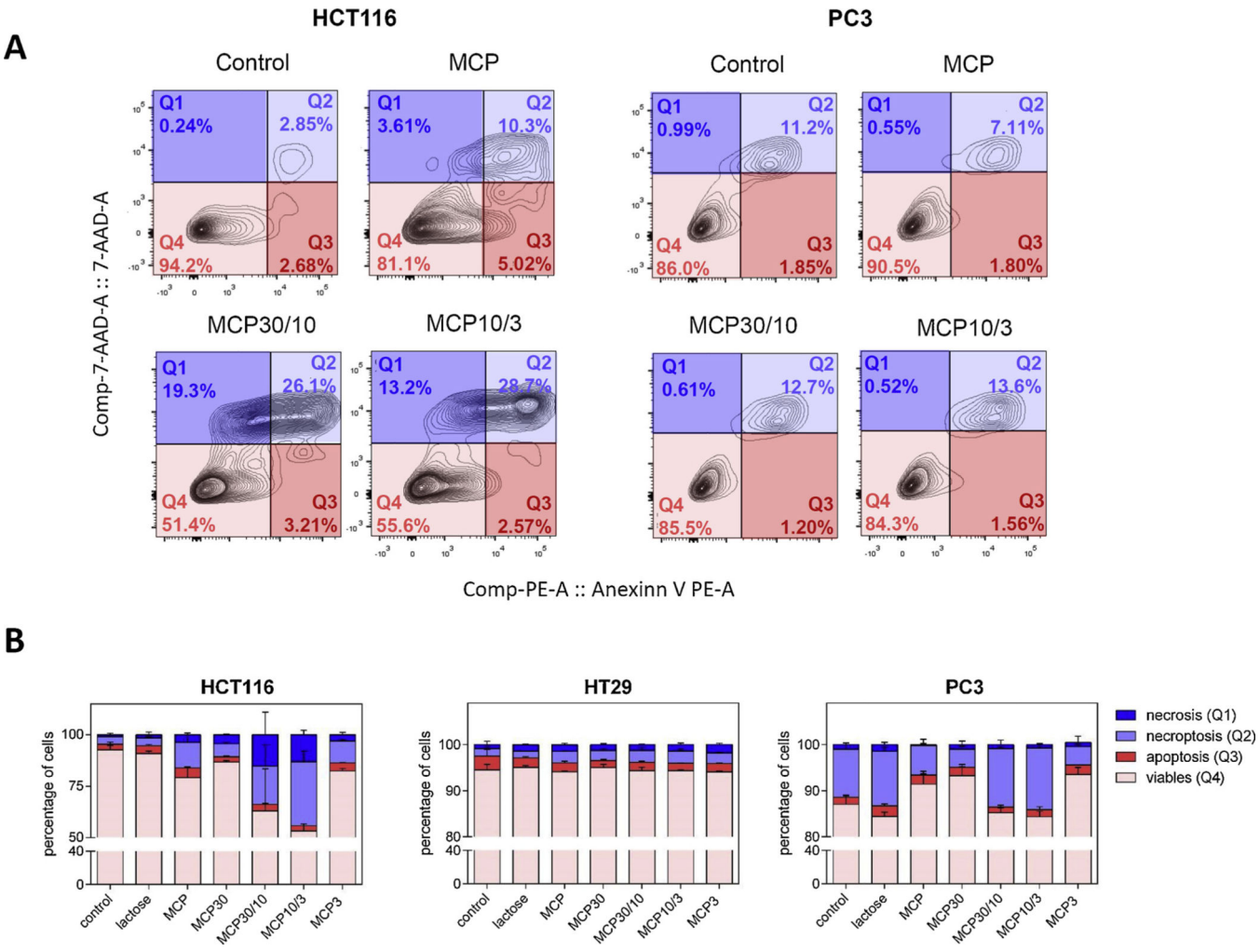

Fig. 4.

Effects of MCP and MCP fractions in HCT116, HT29 and PC3 apoptosis by flow cytometry. Cancer cells were induced to late apoptosis/necroptosis after MCP and MCP fractions treatment for 24 h. **A)** Q1: necrosis quadrant; Q2: necroptosis quadrant; Q3: apoptopsis quadrant; Q4: viable cells quadrant. The most significant differences in graphics are shown in the figure (HCT116 and PC3 cells treatment). **B)** The results were expressed in percentage of cells in comparison with control (no treatment). Results were represented as mean ± SD of two independent experiments, with each performed in triplicate.

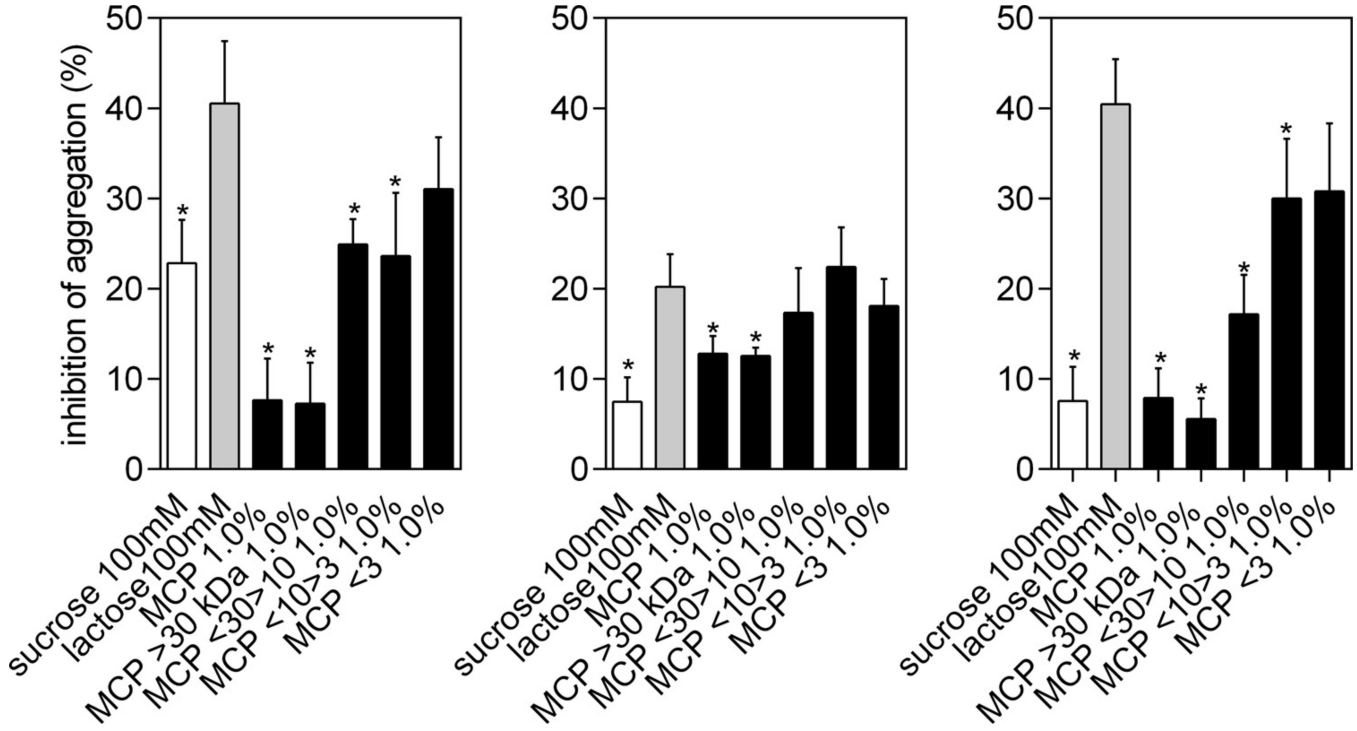

Fig. 5.

Inhibition of homotypic cell aggregation. Data are shown as mean ± SD and the results were expressed in percentage of cells relative to control (with asialofetuin and no treatment). *p < 0.05 vs lactose, according to Dunnett's test.

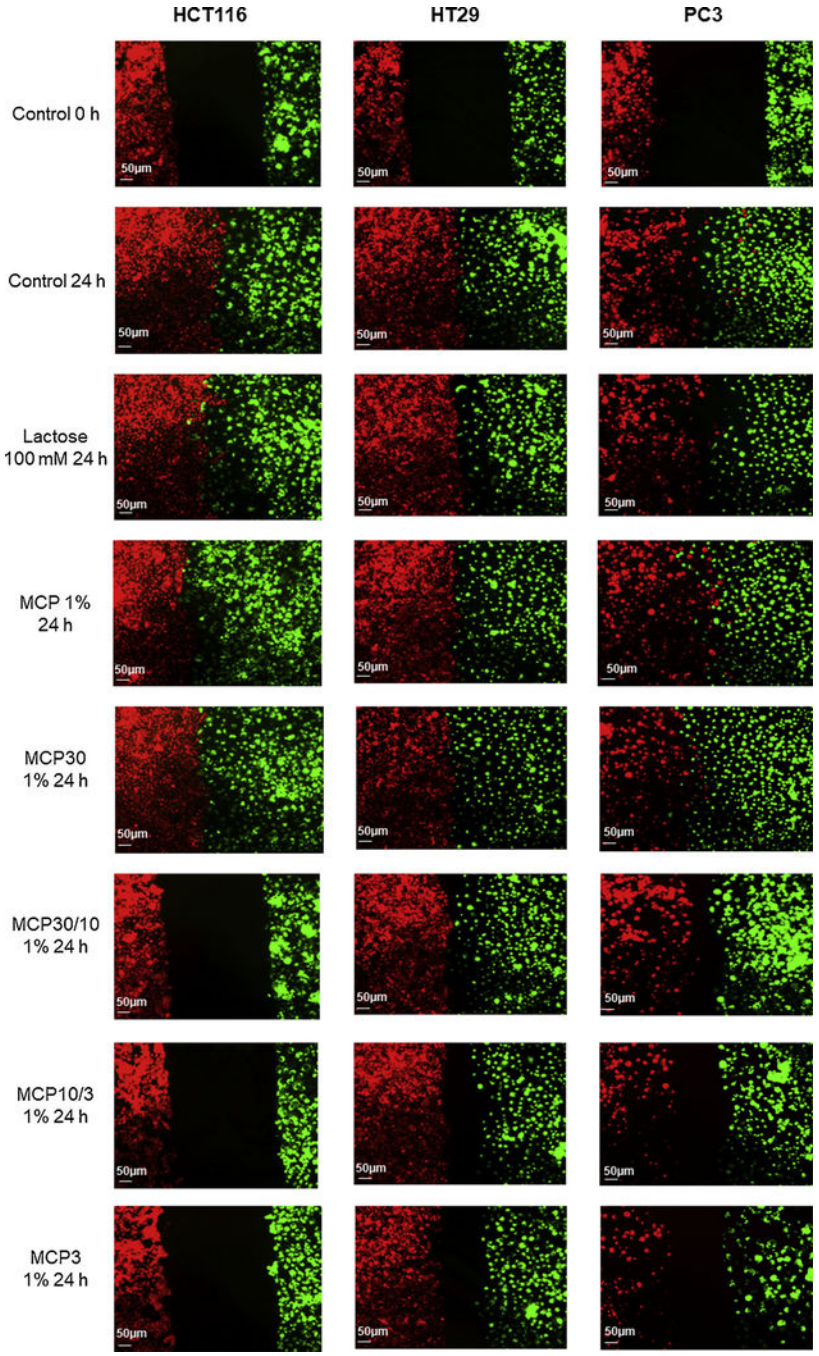

Fig. 6.

Migration assay using endothelial cells (BAMEC) dyed with Dil (red) and cancer cells dyed with DiO (green). Endothelial cells (BAMEC) dyed with DiO (green) and cancer cells dyed with DiI (red). Lower molecular size fractions from MCP had lessen the interaction between cancer cells and BAMEC. Scale bar: 50 μm (For interpretation of the references to colour in this figure legend, the reader is referred to the web version of this article.).

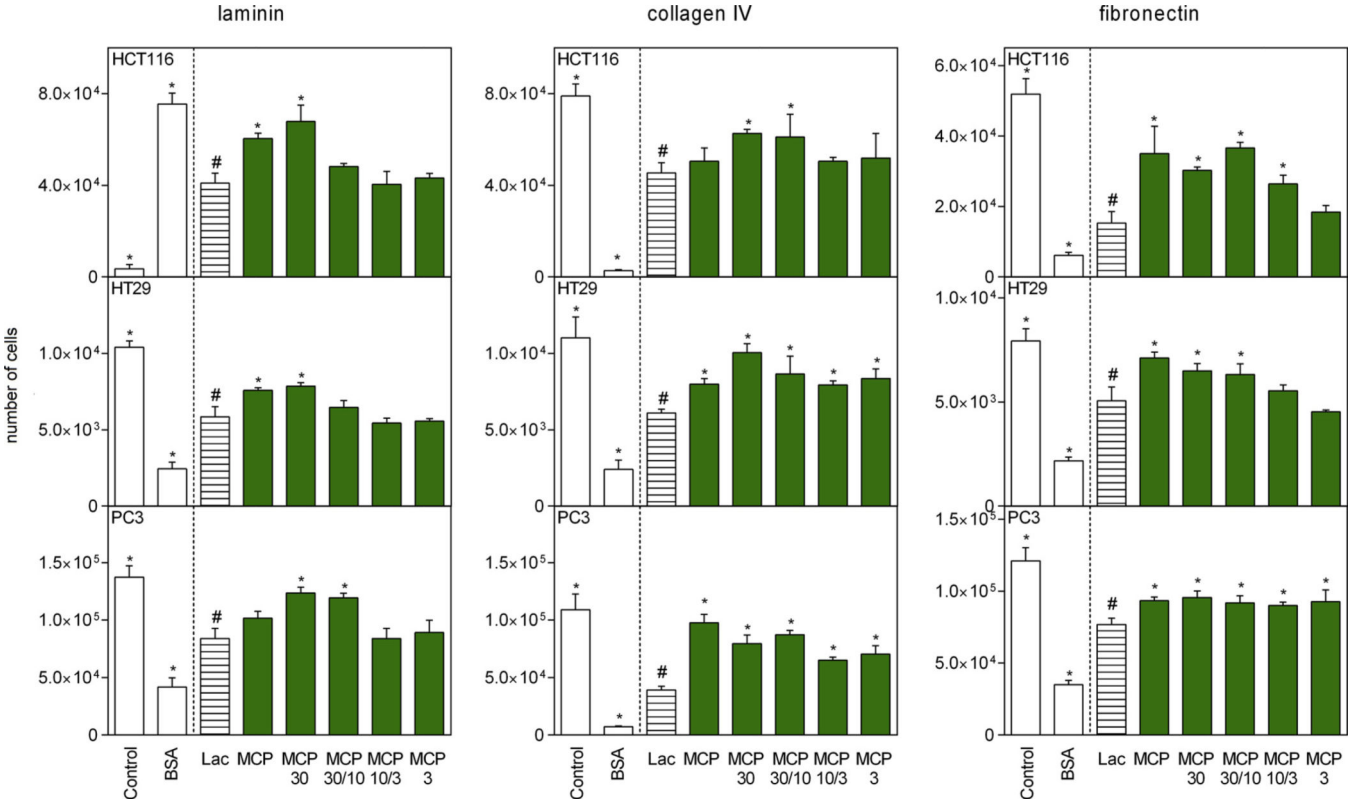

Fig. 7.

MCP and MCP fractions interaction with extracellular matrix proteins (laminin, collagen IV and fibronectin) and cancer cells lines. Data are shown as mean ± SD. All treatments are significant different from control (Dunnett's test). All samples are compared with lactose (#) by Dunnett's test and significant differences ($p < 0.05$) are marked with an asterisk.

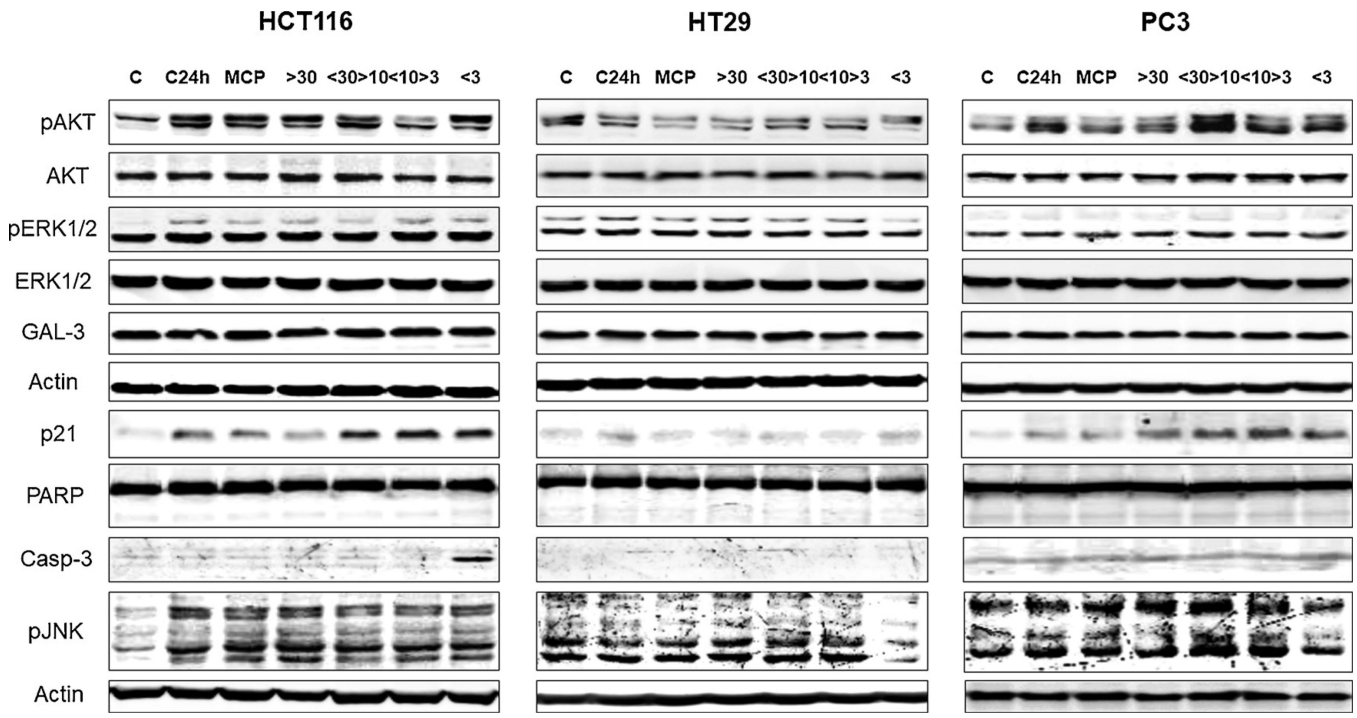

Fig. 8.

Western blotting analysis. Cell lysates were prepared and processed for immunogel blot assay after 24 h of treatment. After BCA assay, equal amounts of proteins were separated using SDS-PAGE. β-Actin was used as the loading control.

Table 1

Molecular size, degree of esterification (DE) and monosaccharide composition of MCP and MCP fractions.

	Monosaccharide composition (g/100g)[a]										
	Molecular size[b]	**DE**[c]	**Rha**	**Fuc**	**Ara**	**Xyl**	**Man**	**Gal**	**GalA**	**Glc**	**GlcA**
MCP	22.2	79.8 ± 4.3	3.1 ± 0.2	0.1 ± 0.0	2.5 ± 0.6	1.5 ± 0.4	0.9 ± 0.2	11.5 ± 1.4	75.8 ± 2.5	1.5 ± 0.4	3.1 ± 0.2
MCP30	35.2	84.2 ± 4.8	3.5 ± 0.2	0.1 ± 0.1	3.2 ± 0.8	1.9 ± 0.5	0.9 ± 0.2	10.8 ± 0.9	74.7 ± 2.5	1.7 ± 0.5	3.2 ± 0.3
MCP30/10	27.5	85.0 ± 5.6	2.7 ± 0.0	0.0 ± 0.0	1.1 ± 0.0	0.5 ± 0.0	0.5 ± 0.0	11.2 ± 0.0	80.0 ± 0.2	1.6 ± 0.2	2.4 ± 0.1
MCP10/3	10.2	78.9 ± 2.1	2.0 ± 0.0	0.0 ± 0.0	0.9 ± 0.1	1.1 ± 0.1	1.4 ± 0.1	20.7 ± 7.8	69.7 ± 7.3	0.7 ± 0.2	3.5 ± 0.4
MCP3	5.1	53.7 ± 6.0	1.7 ± 0.0	0.1 ± 0.0	0.8 ± 0.0	0.6 ± 0.3	1.2 ± 0.1	5.5 ± 0.1	86.0 ± 0.1	1.0 ± 0.2	3.2 ± 0.0

[a] Results represents mean ± SD ($n \geq 7$).

[b] Molecular size is dextran equivalent. The maximum and minimum values at half height for each analysis are represented in Figure S1.

[c] DE: degree of esterification. DE values were calculated using the calibration curve ($R^2 = 0.9798$) and results are expressed in mean ± SD ($n = 3$). GlcA: glucuronic acid; Glc: glucose; GalA: galacturonic acid; Gal: galactose; Man: mannose; Xyl: xylose; Ara: arabinose; Fuc: fucose; Rha: rhamnose. MCP: modified citrus pectin.